Electronic structures and nonlinear optical coefficients of β-BaB_2O_4

W.-D. Cheng,* J.-S. Huang, and J.-X. Lu
Fujian Institute of Research on the Structure of Matter, Chinese Academy of Sciences, State Key Laboratory of Structural Chemistry, Fuzhou, Fujian 350002, People's Republic of China
(Received 9 June 1997)

The electronic structures have been calculated using the INDO/S-CI method, and following combination with the sum-over-sates method the dynamic second-order polarizabilities have been computed for the $Ba_3(B_3O_6)_2$ microspecies of β-BaB_2O_4 (BBO) crystal. Then the second-order susceptibilities of BBO crystal have been obtained in terms of microspecies number density and local-field correction factor. It is found that the top levels of the valence band derive from O $2p$ orbitals and the bottom levels of conduction band derive from Ba orbitals. For the calculation with the basis set containing Ba $5d$, $6s$, and $6p$ valence orbitals, the obtained energy gap of 6.41 eV is in agreement with the experimental value of 6.43 eV. The second-order nonlinear optical coefficient d_{22} is 3.51 pm/V as compared to the observed value of 2.22 pm/V at an incident wavelength of 1064 nm. The dispersion of the frequency-dependent second-order polarizability is larger from the calculations with the basis set containing Ba $6s$, $6p$ orbitals than with the basis set containing Ba $5d$, $6s$, and $6p$ orbitals. The excited-state charge transfer from anion O^{2-} to cation Ba^{2+} makes significant contributions to the nonresonant second-order susceptibility. It is also found that anionic group theory is an unreasonable approximate treatment in calculating the optical gap and the conclusion that the electronic susceptibilities derive from electronic transitions among anionic group $(B_3O_6)^{3-}$ is suspect for BBO crystal. [S0163-1829(98)02703-9]

I. INTRODUCTION

A great number of theoretical and experimental investigations for nonlinear optical crystals β-BaB_2O_4 (BBO) have been made towards understanding the electronic energy-band structures and the sensitive structural unit contributing to optical susceptibility since an inorganic borate compound was found to have a large second-harmonic generation (SHG) signal.[1] The band gap and valence-band structures were determined by vacuum ultraviolet spectroscopy and valence-band x-ray photoemission spectroscopy,[2] and nonlinear optical coefficients were observed.[3] The calculated results of electronic structures, using the *ab initio* pseudofunction (PSF) energy-band method[4] in which the basis set consisted of sp^3 PSF orbitals on the O and Ba atoms and two sets of sp^3 PSF orbitals on the B atom, and using the first-principle orthogonalized linear combination of atomic orbitals (OLCAO) energy-band method based on the local-density approximation[5] in which the basis functions consisted of Ba ([Xe] core plus $6s$, $6p$, and $5d$, $5p$ valence orbitals), B and O ($1s$, $2s$, $2p$, $3s$, and $3p$), showed that an upper valence-band (VB) region derives from O $2p$ orbitals and B-O bonding orbitals, and that a lower VB region originates from B $2s$ and O $2s$ orbitals, and that the bottom of the conduction band (CB) is mainly from the Ba ion orbital. The optical gap for BBO results from a transition from the borate-group-derived orbitals to Ba-derived orbitals, contrary to the findings of the anionic group-theoretical method.[2] The nonlinear optical coefficients have not yet been calculated by the *ab initio* PSF and OLCAO energy-band methods, but have been calculated for BBO crystal by using the anionic group theory.[6] This theory has two assumptions as basic premises: (i) the overall SHG coefficient of the crystal is the geometrical superposition of the microscopic second-order polarizability tensors of the relevant ionic groups, and has nothing to do with the essentially spherical cations; (ii) the microscopic second-order polarizability of the basic anionic group can be calculated from the localized molecular orbitals of this group using quantum-chemistry calculation methods.[7] Under these assumptions the state wave function of the system does not have any contributions from cation orbitals. As a result, the hypothesis may well break down when dealing with several problems not considered in the anionic group theory. For example, the anionic group theory does not work for the calculations of electronic transition dipole moments from the ground state (or excitation state) to excitation states containing some components of the cation orbitals. As is well known, the second-order polarizability in the context of the sum-over-states (SOS) is governed not only by the transition energy in the denominator, but also by the product of the transition dipole moments in the numerator. Consequently, it is a question for the conclusion[6] of which the second-order nonlinear optical coefficients of BBO crystal is mainly the contributions from the electronic transition among the anionic group.

In order to understand the electronic origin of the optical properties and determine the sensitive structural unit contributing to susceptibility, the electronic structures and the second-order susceptibilities of BBO are calculated for the basis functions on the Ba containing the $6s$, $6p$, and the $5d$, $6s$, and $6p$ valence orbitals, respectively, in terms of the INDO/CI and following combination with the SOS method. This method is demonstrated to be successful in calculating the susceptibilities of organometallic compounds and inorganic solid compounds.[8–11] The calculated band structures show that the top levels of the valence band contribute from the O $2p$ orbitals and the bottom levels of the conduction-band contribute from the Ba orbitals, and band gap is 6.28 and 6.41 eV for the different basis functions on the Ba, re-

spectively. The calculated averaged second-order polarizability β_{av}, which is independent of the direction, mostly derives from the excited-state charge transfer from the O $2p$ orbitals to Ba $6s$ orbital; the calculated second-order polarizability, β_{333}, mainly derives from the excited-state charge transfer from the O $2p$ orbitals to Ba $5d$, $6p$ orbital for $Ba_3(B_3O_6)_2$ microspecies of BBO crystals. The second-order susceptibility of BBO crystal is obtained by the second-order polarizability superposition and local-field correction of the microspecies.

II. COMPUTATIONAL PROCEDURES

The electronic structural calculations of isolated molecules (microspecies of the BBO crystal), are based on an all-valence-electron, semiempirical INDO self-consistent field (SCF) molecular-orbital (MO) procedure with configuration interaction (CI) modified by Zerner and co-workers.[12–15] The one-center core integral $U_{\mu\mu}$, resonance integral β_{μ}, two-electron integral $\gamma_{\mu\nu}$, overlap integral $S_{\mu\nu}$, and density-matrix element $P_{\mu\nu}$ are involved in the matrix element of Fock operator under the INDO approximation. The INDO model as employed herein includes all one-center two-electron integrals, and two-center two-electron integrals $\gamma_{\mu\nu}$. The one-center two-electron integrals $\gamma_{\mu\mu}$ are chosen from the Pariser approximation,[16] and the two-center two-electron integrals are calculated using the Mataga-Nishimoto formula[17] in the spectroscopic version of the INDO method. In order to show the contribution of Ba $5d$ orbital the two types of basis functions are involved in present calculations. One is the O $2s$, $2p$ and the B $2s$, $2p$ as well as the Ba $6s$, $6p$ orbitals; the other is the O $2s$, $2p$ and B $2s$, $2p$ as well as Ba $5d$, $6s$, $6p$ orbitals. The Slater orbital exponents ζ and the other calculating parameters can be found in Ref. 18. The MO calculations were performed using the restricted Hartree-Fock INDO method. The ground state, which is obtained from the calculated results of the SCF, is taken as the reference state in the CI. Only single-substituted determinants relative to the ground-state configuration are considered and only singlet spin-adapted configurations need to be included in the CI calculations. The determinant wave functions can be expressed as

$$\Phi_{\mathrm{CIS}}=a_0\phi+\Sigma\Sigma a_{i\to b}\phi_{i\to b}. \tag{1}$$

Here the subscripts i,b, take on values of 1–12 in this study. This means that an electron is promoted from the 12 highest occupied orbitals to the 12 lowest unoccupied orbitals and configuration space is constructed from these 24 active orbitals. The coefficients a are varied to minimize the expected value of the energy, leading to the equations

$$\Sigma(H_{ij}-E_k\delta_{ij})a_{ij}=0, \quad j=0,1,2,\ldots, \tag{2}$$

where the H_{ij} are configurational matrix elements and E_k are energy elements. The excited states correspond to the configuration interaction wave functions Φ_{CIS} with higher energy roots E_k $(k>0)$. The energy difference between the excited state and ground state is defined as the electron transition energy. The dipole and transition moment matrix elements are expressed as a sum of one-electron integrals.[19] The oscillator strength is evaluated with the dipole length operator, maintaining all one-center charge and polarization terms in the CI calculations. Higher-order correlations are neglected since their influence is taken into account through the choice of semiempirical two-electron integrals γ and empirical resonance β.

The tensor components of the frequency-dependent second polarizability $\beta(-2\omega;\omega,\omega)$ of microspecies are calculated by the SOS method.[20,21] The compact expressions of β can be written as follows:

$$\beta_{ijk}(\omega_\sigma;\omega_q,\omega_p)=1/\hbar^2 P_f\Sigma_{mn}\mu^i_{gn}\mu^j_{nm}\mu^k_{mg}[(\omega_{ng}-\omega_\sigma)\times(\omega_{mg}-\omega_p)]^{-1}, \tag{3}$$

where $\omega_p=\omega_q=\omega$, $\omega_\sigma=-2\omega$. P_f is a full permutation operator by which the Cartesian indices are to be permuted along with the over input and output frequencies. The β is governed not only by the state energy in the denominator, but also by the product of transition dipole moments in the numerator. The detail expression for $\beta(-2\omega;\omega,\omega)$ can be found in the literature.[8] The excited energies, and transition dipole moments in Eq. (3) can be obtained from the calculated results using the INDO/S-CI method. How many excited states are included in computing β depends on the convergence of the summations in the series of the SOS method. The convergences obtained are about 120 excited states for tensor β and the summations are over 170 states in the SOS. For each microspecies in the material, we can relate each element of the tensor for the macroscopic second-order electric susceptibility χ_{IJK} to the microscopic second-order polarizability B_{IJK} by

$$\chi_{IJK}=Nf_I(\omega_1)f_J(\omega_2)f_K(\omega_3)B_{IJK}. \tag{4}$$

In this formula, the subscripts I,J,K refer to axes in the laboratory-fixed coordinate system, N is the species number density, and $f_I(\omega_i)$ is the local field factor at radiation frequency ω_i. The microscopic second-order polarizability B_{IJK} in laboratory-fixed coordinates is related to the molecule-fixed coordinate system by

$$B_{IJK}=\Sigma_{ijk}C_{Ii}C_{Jj}C_{Kk}\beta_{ijk}, \tag{5}$$

in which C_{Ii} is the direction cosine between the laboratory-fixed I axis and the molecule-fixed i axis, and β_{ijk} is an element of the microscopic second-order polarizability tensor. The second-order polarizability averaged over all orientations of the individual species is accessible in an approximate treatment. However, in the case of single crystals, it is possible to determine individual elements of the second-order polarizability tensor.

The calculations of the second-order susceptibilities of BBO crystal is based on the cluster model. The microspecies $Ba_3(B_3O_6)_2$ with C_{3v} symmetrical group is selected as a microstructural unit in the BBO crystal, as shown in Fig. 1. This crystal belongs to the space group $R3c$ with unit-cell parameters $a=8.380$ Å, $\alpha=96.65°$.[22] The average distances are $r(\text{B-O}_{\text{terminal}})=1.332$, $r(\text{B-O}_{\text{ring}})=1.397$, $r(\text{Ba-O})=2.818$ Å for BBO. The electronic structures and microscopic polarizabilities of the microstructural unit of BBO crystal are calculated using the crystallographic data.

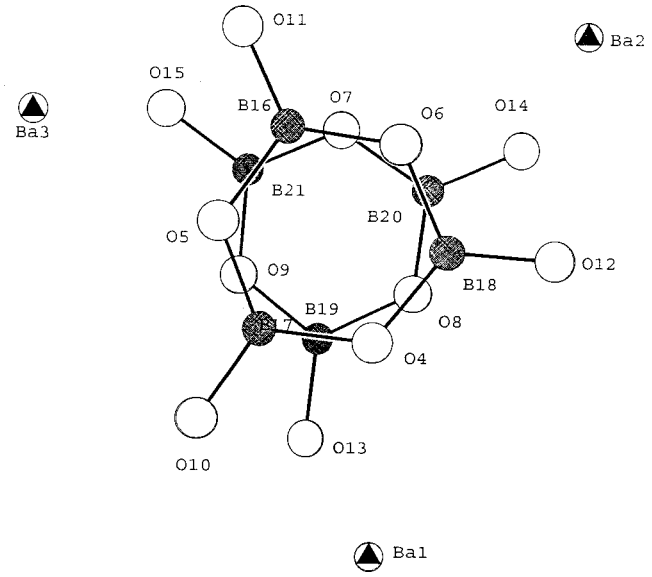

FIG. 1. The structure of selected microspecies $Ba_3(B_3O_6)_2$ of BBO crystal.

III. RESULTS AND DISCUSSIONS

Most properties of materials represent the response of material to some external electromagnetic field or mechanical force, and the physical properties from experimental observation can be described by electronic state wave functions. Furthermore, the features of electronic structure represent directly the response of the electronic states to an electromagnetic field. So it will be helpful for investigation of the electronic structures of BBO to discuss their optical properties.

A. Electronic structures

Case A for which the Ba valence orbitals only include the 6s, 6p orbitals

The calculations of electronic structures are based on the INDO/S quantum chemical method. The calculated energy bands are divided into four zones for the $Ba_3(B_3O_6)_2$. The zone of energy below -24.0 eV is a lower valence band and this zone is attributable to the $2s$ orbitals of oxygen and boron atoms. There are 63–79 % O $2s$ orbital character and 3–15 % B $2s$ orbital character in this zone. It is approximately assigned as an s valence band. The second zone from -11.8 to 0.00 eV contributes from 56%–98% O $2p$ orbital character, but mixing with $<34\%$ B $2p$ orbital character makes it an upper valence band. These two band zones are fully occupied by electrons. The closer the top edge of the VB, the more contributions are from the O $2p$ orbitals. The atomic-state density of the upper VB zone, i.e., the calculated second zone, is displayed in Fig. 2(a). It is found on the left side of Fig. 2(a) that the three peaks localized in the energies -12.0 to -6.0 eV can be assigned as the σ-bonding interactions between the O $2p$ and B $2p$ orbitals, and the two peaks localized in the energies -5.5 to -3.0 eV can be assigned as π-bonding interactions between the O $2p$ and B $2p$ orbitals, and that the two peaks localized in the energies -1.9 to -0.6 eV are assigned as the $2p$ nonbonding orbitals of the terminal oxygen ($2p$-orbital contributions $>92\%$). The third zone is a lower CB and its atomic state

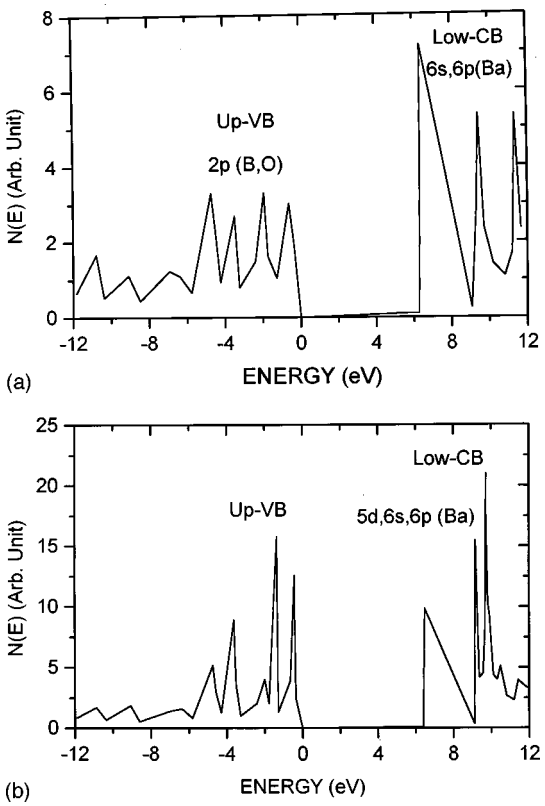

FIG. 2. Atomic state density, (a) containing Ba $6s$, $6p$ orbitals and (b) containing Ba $5d$, $6s$, $6p$ orbitals.

density is shown on the right side of Fig. 2(a). The peaks localized in the energy region between 6.40 and 9.50 eV are all the contributions from the barium ionic state ($>83\%$). The fourth zone from 10.20 to 22.34 eV is made up of the antibonding interactions between the boron and oxygen atomic valence orbitals. The last two zones are completely empty ones. It is noted that these assignments for atomic states are only a general trend. From Fig. 2, it is found that the calculated energy gap between the upper VB and lower CB is 6.28 eV, and this value is to be compared with the measured optical gap of 6.43 eV.[2]

Case B for which the Ba valence orbitals include the 5d, 6s, 6p orbitals

The calculated electronic energy band is divided into VB and CB regions. The VB region is completely occupied and the atomic states of the anionic group $(B_3O_6)^{3-}$ make the most contributions to the VB. This situation is the same as for case A. The lower CB, however, has different contributions from case A. Its atomic state density is shown on the right side of Fig. 2(b). The peak localized in the energy of 6.50 eV is the contribution from 84% Ba $6s$ orbital character, and peaks localized in the energy region between 9.17 and 10.33 eV are the contributions from the 47–99 % Ba $5d$ orbital character. The upper CB zone from 10.50 to 22.37 eV is made up of the antibonding interactions between the boron and oxygen atomic valence orbitals. The calculated energy gap is 6.41 eV and this value is an excellent agreement with the measured optical gap of 6.43 eV.[2]

The calculated electronic occupied numbers of the Ba atomic orbitals by Mulliken analysis are listed in Table I.

TABLE I. The occupied number (e) of Ba atomic orbitals and β (10^{-30} cm^5 esu^{-1}) cumulative values of nonlinear polarizability of $Ba_3(B_3O_6)_2$ at input wavelength of 1064 nm.

State	$6s$	$6p$	Ba	β_{333}	β_{av}	$6s$	$6p$	$5d$	Ba	β_{333}	β_{av}
1	0.11	0.46	0.57			0.10	0.43	0.10	0.63		
2	0.42	0.57	0.99	0.00	0.00	0.42	0.54	0.10	1.06	0.02	0.02
3	0.42	0.57	0.99	0.00	0.88	0.41	0.55	0.10	1.06	0.02	0.80
4	0.42	0.58	1.00	0.01	1.57	0.41	0.55	0.10	1.06	0.02	1.32
5	0.42	0.58	1.00	0.05	1.62	0.41	0.55	0.10	1.06	0.03	1.32
6	0.42	0.58	1.00	0.06	1.65	0.41	0.55	0.10	1.06	0.03	1.38
36	0.42	0.58	1.00	0.09	2.43	0.41	0.55	0.10	1.06	0.06	1.99
52	0.13	0.81	0.94	0.78	3.73	0.13	0.68	0.24	1.05	0.58	3.05
99	0.13	0.71	0.84	1.26	4.88	0.13	0.68	0.22	1.03	1.06	4.08
170	0.13	0.54	0.67	1.62	5.97	0.12	0.53	0.39	1.04	1.21	4.34

Even though these data are not absolute, the relative values are available. From these values we can calculate the atomic net charges. In this way, the calculated electronic structures of the $Ba_3(B_3O_6)_2$ on the ground state show a basic chemical picture of BBO crystal, like an ionic solid one. In this chemical picture, the formation of BBO from its components involves the transfer of electrons from Ba, which is left in crystal as the cation $Ba^{1.4+}$, to the group B_2O_3, which is left in the crystal as anion group $(B_3O_6)^{2.1-}$. However, those on the low-lying excitation states show the same covalent solid features (ionic interaction reduction) for which the Ba in the crystal is as the cation $Ba^{0.9+}$ and the B_2O_3 in the crystal is as the anionic group $(B_3O_6)^{1.4-}$. Comparing the Ba charges on the excited states with the ground state, we can show that the Ba ion gained more electrons from the anionic group $(B_3O_6)_2{}^{3-}$ and the electronic delocalization of $Ba_3(B_3O_6)_2$ is larger on the excited states than on the ground state.

B. Nonlinear optical coefficients

Optical properties of crystalline state can be thought of as being built up from the corresponding properties of individual molecules or microspecies, and susceptibility of bulk has a relation with the polarizability of microspecies. Therefore, macroscopic nonlinear susceptibility of material can be calculated by giving the nonlinear polarizability of microspecies, local-field correct factor, and molecular number density. Recently, the electric-dipole second polarizability β and the more complicated hyperpolarizability governing the higher-order contributions to SHG, and environmental effects on the response, have been included in the treatment of nonlinear optical phenomena.[23] In the present study, we only consider the leading contribution to SHG coming from electric dipole oscillation at 2ω quadratic in the electric field at ω.

Nonlinear optical coefficients of microspecies $Ba_3(B_3O_6)_2$

For the $Ba_3(B_3O_6)_2$ under the present consideration, we take it as C_{3v} symmetric structure, as shown in Fig. 1. In this symmetry the β tensor consisting of 27 Cartesian components is left for 11 nonzero tensor elements. In low-frequency region Kleinman symmetry[24] can be used to simplify further the relationship of the tensor components and the independent tensor components will be only three elements. The calculated β tensor elements for case A (Ba with $6s$, $6p$ valence orbitals) and case B (Ba with $6s$, $6p$, $5d$ valence orbitals) are listed in Table II at $\hbar\omega = 1.165$ and 0.00 eV, respectively. From these values of Table I, it is found that the above-mentioned relations are approximately established. The calculated value of $\beta_{111} \cong 0.0$ and the independent elements are only β_{333}, β_{222}, and β_{311} at $\hbar\omega = 0.00$ eV. The values of the β elements are generally larger for the calculations of case A than case B. In the following discussions an averaged second-order polarizability β_{av} is defined as

$$\beta_{av} = \left(\sum_i \beta_i^2 \right)^{1/2} \quad \text{and} \quad \beta_i = \beta_{iii} + \tfrac{1}{3} \sum_{j \neq i} (\beta_{ijj} + \beta_{jij} + \beta_{jji}). \tag{6}$$

Before attempting to compute the variation of the second-order polarizability versus frequency for $Ba_3(B_3O_6)_2$, it is

TABLE II. The nonlinear polarizability β (10^{-30} cm^5 esu^{-1}) elements of $Ba_3(B_3O_6)_2$.

Element	333	222	211	121	112	311	131	113	322	232	223
Ba,sp[a]	1.32	0.64	−0.63	−0.63	−0.63	1.42	1.42	1.42	1.46	1.46	1.46
Ba,sp[b]	1.62	0.14	−0.17	−0.17	−0.17	1.67	2.38	2.38	1.73	2.43	2.43
Ba,dsp[a]	1.01	0.47	−0.54	−0.54	−0.54	1.00	1.00	1.00	0.94	0.94	0.94
Ba,dsp[b]	1.21	0.11	−0.16	−0.18	−0.18	1.29	1.76	1.76	1.20	1.68	1.68

[a]Input zero frequency.

[b]Incident wavelength of 1064 nm.

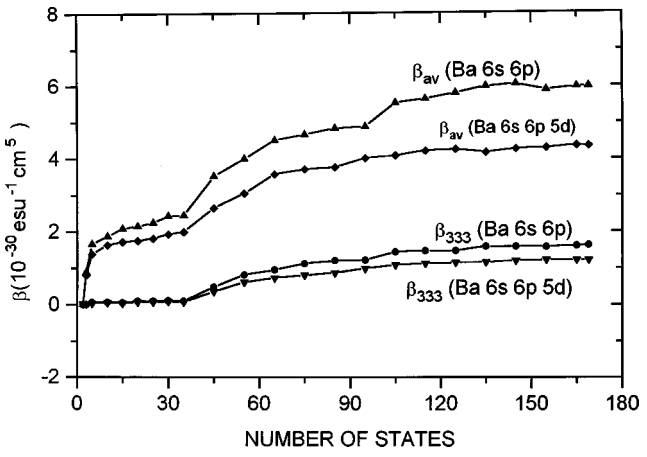

FIG. 3. The second-order polarizability of microspecies at $\lambda = 1064$ nm.

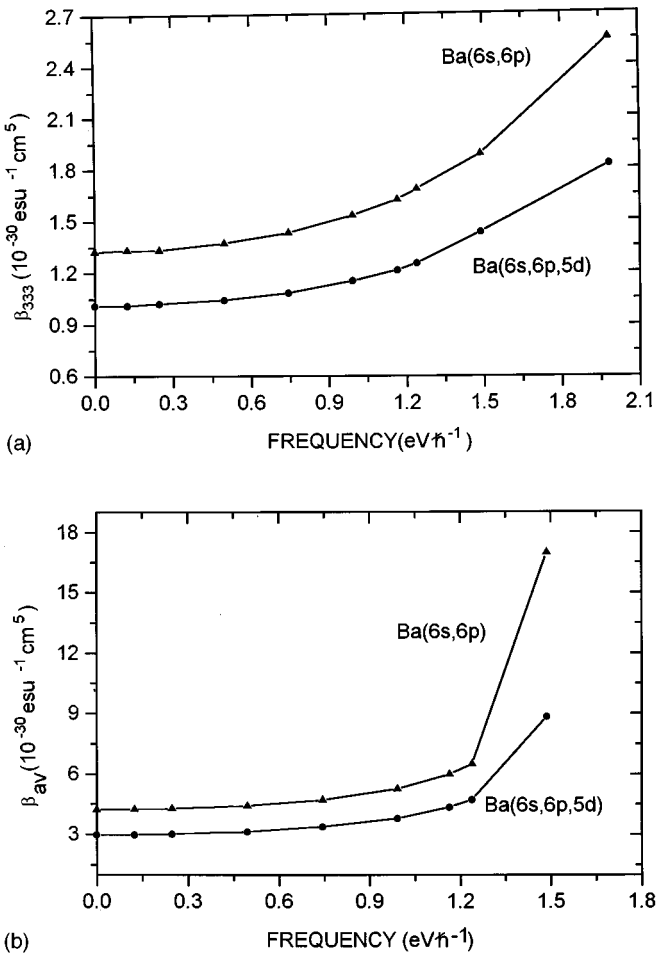

FIG. 4. Frequency dependence of (a) β_{333} and (b) $\beta_{\rm av}$ for microspecies.

necessary to investigate the behavior of the convergence in the summation of states and to determine whether the results calculated from the INDO/S-CI method are reliable. Figure 3 shows the plots of the calculated $\beta_{\rm av}$ and β_{333} versus the number of states for the microspecies of BBO crystal at $\lambda = 1064$ nm ($\hbar\omega = 1.165$ eV). Table I lists the calculated occupied number of Ba $6s$, $6p$, and $5d$ valence orbitals and the cumulative values of $\beta_{\rm av}$ and β_{333} in some states. As shown in Eq. (3), the value of β is proportional to the product of transition dipole moments with a given transition energy. From the transition moment elements, we can identify specific virtual excitation processes among the eigenstates of the system that make the most significant contributions to β. Furthermore, the eigenstate is constructed by Eq. (1) and the configuration is constructed by the occupied orbitals (basic functions are for atomic orbitals). From compositions of the configurations and orbitals, we can identify the specific atomic states making the major contributions to β. Consequently, an analysis for $Ba_3(B_3O_6)_2$ can be obtained by combination of Table I with Fig. 3. It is found that the convergence of $\beta_{\rm av}$ and β_{333} is reached after summation over 120 states. The $\beta_{\rm av}$, β_{333} obtained from summation over 36 states is about 46%, 5% of the $\beta_{\rm av}$, β_{333} obtained from summation over 170 states for case A, and is about 41%, 6% for case B, respectively. Comparing the atomic-orbital occupied number of excited states with that of ground state (state 1), it is shown that the Ba $6s$ orbital below state 36 obtains more charges and Ba $6p$, $5d$ orbitals above state 37 obtain more charges from the anion group $(B_3O_6)^{3-}$ in the BBO crystal. The $\beta_{\rm av}$, β_{333} obtained from summation over about 100 states is about 94%, 88% of the $\beta_{\rm av}$, β_{333} obtained from summation over 170 states for case B, and that is about 82%, 78% for case A, respectively. It is found from Table I that the Ba $5d$, $6s$, $6p$ orbital populations and the β values have large variations between states 36 and 52. This is due to the fact that some states have larger contributions. For instances, the 40th state has the greatest contribution from the configuration $\phi_{48\to54}$ (47%). This configuration is formed by an electron from HOMO (the 48th molecular orbital, φ_{48}) composed of 90% O $2p$ orbital, to the orbital φ_{54} composed of 60% Ba $6p$ and 30% Ba $5d$ orbital; the 52nd state has the major contributions from the configurations $\phi_{45\to57}$ (23%) and $\phi_{43\to56}$ (16%). The configuration $\phi_{45\to57}$ is constructed by one electron from the orbital φ_{45} composed of 72% O $2p$ orbital, to the orbital φ_{57} composed of 57% Ba $6p$ and 36% Ba $5d$ orbital. Moreover, in view of the atomic state density of the upper VB and lower CB as well as the Ba atomic-orbital occupied number, it can be stated that the excited-state charge transfers from the O $2p$ orbital to the Ba $6s$ orbital make the dominate contributions to the averaged second-order polarizability, $\beta_{\rm av}$, which is the independent of direction, and that the excited-state charge transfers from the O $2p$ orbital to the Ba $5d$ or $6p$ orbital make significant contributions to the second-order polarizability, β_{333}, which is dependent on direction. The calculated frequency dependence of $\beta_{\rm av}$ and β_{333} for cases A and B are plotted in Fig. 4. The curves appear as a small dispersion in the low-frequency region ($\hbar\omega$ is below 1.20 eV). The $\beta_{\rm av}$ cures show a preresonance at magnitudes of 6.49×10^{-30} and 4.72×10^{-30} cm^5 esu^{-1}, and the β_{333} cures show preresonance at 1.60×10^{-30} and 1.88×10^{-30} cm^5 esu^{-1} for cases A and B, respectively. Away from resonance, at 1.165 eV, the $\beta_{\rm av}$ values are 5.97×10^{-30}, 4.34×10^{-30} cm^5 esu^{-1}, and β_{333} values are 1.62×10^{-30}, 1.21×10^{-30} cm^5 esu^{-1} for cases A and B, respectively. By comparing case A with B, we find the variation of the second-order polarizability β versus

TABLE III. The parameters for calculating nonlinear susceptibility of BBO at 1064 nm and NLO coefficients. The values in the parentheses are the observed ones.

Case	N[a]	F_{YYY}	F_{ZZZ}	F_{ZXX}	B_{YYY}[b]	B_{ZZZ}	B_{ZXX}	χ_{YYY}[c]	χ_{ZZZ}	χ_{ZXX}	d_{22}[c]	d_{31}
Ba,sp	3.466	3.998	3.139	3.677	1.62	−0.14	0.17	9.40	−0.64	0.91	4.70	0.46
Ba,dsp	3.466	3.998	3.139	3.677	1.21	−0.11	0.16	7.02	−0.50	0.85	3.51 (2.22)	0.43 (0.16)

[a]For 10^{21} cm^{-3}.
[b]For 10^{-30} cm^5 esu^{-1}.
[c]For pm/V.

frequency is sharper for the former than the latter in the high-frequency region.

Nonlinear optical coefficients of BBO crystal

The macroscopic second-order electric susceptibility χ of the BBO crystal can be calculated by Eq. (4). In this equation, N is obtained from the product of mass density D and Avogadro's constant L, divided by the molar mass M, i.e., $N=L\times D/M$. For $Ba_3(B_3O_6)_2$, with a formula mass of 668.87 g/mol and a mass density of 3.85 g/cm^3,[22] we obtain $N=3.466\times10^{21}$ cm^{-3}. In Eq. (4) the local field factor $f_I(\omega_i)$ can be estimated under an approximation of homogeneous medium[25] by

$$f_I(\omega_i)=[\varepsilon_I(\omega_i)+2]/3=[n_I(\omega_i)^2+2]/3, \qquad (7)$$

where $\varepsilon(\omega_i), n(\omega_i)$ are the dielectric constant and index of refraction for the medium at frequency ω_i, respectively. The Lorentz field (i.e., local field)[25] has as its source all external charges and the dipole fields of all microspecies in the bulk material other than the microspecies for which local field is to be calculated; that is, the interactions among microspecies and an influence of the surrounding environment upon the microspecies. In the local field developed by Munn[23] the microspecies in bulk material is not only subjected to an induced electric field, but also subjected to a magnetic induction. This is a precise treatment of the local-field correction of microspecies. F_{IJK} listed in Table III are obtained from the relation, $F_{IJK}=f_I(2\omega)f_J(\omega)f_K(\omega)$, and $f_I(\omega)$, as written in Eq. (7), is calculated in terms of the observed refractive index.[26] The transformation coefficients of Eq. (5), C, are only 0, 1, and −1. This is because the space structures of both the BBO crystal and the selected $Ba_3(B_3O_6)_2$ microspecies are of a C_{3V} symmetrical group and the direction cosine between the laboratory-fixed axis and the microspecies-fixed axis are only the three values cos 0°, cos 90°, and cos 180°. In laboratory-fixed coordinates, therefore, the second-order polarizability of the $Ba_3(B_3O_6)_2$, B_{YYY}, is β_{333}, and B_{ZXX} is $-\beta_{211}$. By inserting the necessary values into Eq. (4), we can obtain values of the macroscopic second-order susceptibility χ of the BBO crystal. For example, B_{YYY} is 1.21×10^{-30} cm^5/esu at an incident light wavelength of 1064 nm; N is 3.466×10^{21} cm^{-3}; F_{YYY} is 3.998. We derive χ_{YYY} of 16.76×10^{-9} esu for BBO crystal and the corresponding d_{22} ($d=\chi/2$) value is 3.51 pm/V (8.38×10^{-9} esu). Both the calculated and observed values[2] of d are listed in Table III. It is found that the theoretical values are close to the observed ones for the second-order susceptibility of the BBO crystal, in particular, the d value calculated based on the basis set containing the Ba $5d$, $6s$, $6p$ orbitals in the calculations is an agreement with the observed value ($d_{22}=2.22$ pm/V).

IV. CONCLUSION

The calculated electronic structures show the basic chemical picture is an ionic solid for the ground state and some covalent solid for the low-lying excited states for the BBO crystal. The calculated VB is divided into the lower VB and upper VB regions. The lower VB derives from O $2s$ and B $2s$ orbitals. The upper VB derives from the bonding interactions between O and B $2p$ orbitals and nonbonding $2p$ orbitals of terminal O. The calculated spectrum of the upper VB reproduces the observed one and is similar to the calculated result from the OLCAO or *ab initio* band methods for BBO. The CB is again divided into the lower CB and upper CB regions. The lower CB derives from Ba ionic states and the upper CB derives from the antibonding interactions between O and B $2p$ orbitals. There are larger contributions from the more electronegative O atom in the VB and the more electropositive B atom in the CB. The calculated energy gap of 6.41 eV is well in agreement with the observed optical gap of 6.43 eV. By comparison of the calculated dynamic second-order polarizabilities the optical dispersion is smaller for the calculation based on the basis set containing the Ba $5d$, $6s$, $6p$ orbitals than that containing the Ba $6s$ and $6p$ orbitals. The calculated nonlinear optical coefficients d_{22} and d_{31} are 3.51 and 0.43 pm/V as compared to experimental values of 2.22 and 0.16 pm/V,[2,26] respectively. The excited-state charge transfers from anion O^{2-} to cation Ba^{2+} make the dominant contributions to the second-order susceptibility in view of the analysis from the orbital character of the top VB and bottom CB regions. The borates of $M(B_3O_5)$ ($M=$Li, Cs) (Refs. 27 and 28) and $LiCs(B_3O_5)_2$ (Ref. 29) have been found to have ultraviolet nonlinear optics. They have a different local bonding structure with BBO. In the former, each borate has both a tetracoordinate and tricoordinate boron atom in anion group, and the electronic origin contributing to nonlinear optical response will be investigated soon.

ACKNOWLEDGMENTS

This investigation was supported by the National Science Foundation of China, the Key Fundamental Foundation of the Chinese Academy of Sciences, and the Foundation of State Key Laboratory of Structural Chemistry. We would like to thank Professor Q.-E. Zhang and J.-K. Liang for beneficial suggestions and Dr. J.-T. Chen for plots in preparing the manuscript.

*Author to whom correspondence should be addressed.
[1] C.-Z. Chen, D.-S. Gao, and C.-T. Chen, Academic Thesis Conf. Cryst. Growth Mater. (China) **B44**, 107 (1979).
[2] R. H. French, J. W. Lin, F. S. Ohuchi, and C. T. Chen, Phys. Rev. B **44**, 8496 (1991).
[3] Y. X. Fan *et al.*, IEEE J. Quantum Electron. **QE-25**, 1196 (1989).
[4] W. Y. Hsu and R. V. Kasowski, J. Appl. Phys. **73**, 4101 (1993).
[5] Y.-N. Xu, W. Y. Ching, and R. H. French, Phys. Rev. B **48**, 17 695 (1993).
[6] R.-K. Li and C. T. Chen, Acta Phys. Sin. **34**, 823 (1985).
[7] C.-T. Chen, Y.-C. W, and R.-K. Li, Int. Rev. Phys. Chem. **8**, 65 (1989).
[8] D. R. Kanis, M. A. Ratner, and T. J. Marks, J. Am. Chem. Soc. **114**, 10 338 (1992).
[9] S. D. Bella, M. A. Ratner, and T. J. Marks, J. Am. Chem. Soc. **114**, 5842 (1992).
[10] W.-D. Cheng, J.-T. Chen, J.-S. Huang, and Q.-E. Zhang, Chem. Phys. Lett. **261**, 66 (1996).
[11] W.-D. Cheng, J.-T. Chen, J.-S. Huang, and Q.-E. Zhang, J. Chem. Soc. Faraday Trans. **92**, 5073 (1996).
[12] A. D. Bacon and M. C. Zerner, Theor. Chim. Acta **53**, 21 (1979).
[13] M. C. Zerner *et al.*, J. Am. Chem. Soc. **102**, 589 (1980).
[14] W. P. Anderson, W. D. Edwards, and M. C. Zerner, Inorg. Chem. **25**, 2728 (1986).
[15] W. P. Anderson, T. R. Cundari, and M. C. Zerner, Int. J. Quantum Chem. **39**, 31 (1991).
[16] R. Pariser, J. Chem. Phys. **21**, 568 (1953).
[17] N. Mataga and K. Nishimota, Z. Phys. Chem. (Munich) **13**, 140 (1957).
[18] The input parameters are as follows. Slater exponents: Ba, $\zeta_{6s,6p}=1.263$ Å^{-1}, $\zeta_{5d}=2.658$ Å^{-1}; B, $\zeta_{2s,2p}=1.300$ Å^{-1}; O, $\zeta_{2s,2p}=2.275$ Å^{-1}. Valence state ionization energies: Ba, $I_{6S}=-5.21$ eV, $I_{6p}=-3.43$ eV, $I_{5d}=-3.22$ eV; B, $I_{2s}=-14.05$ eV, $I_{2p}=-8.70$ eV; O, $I_{2s}=-32.90$ eV, $I_{2p}=-17.28$ eV. Coulomb repulsion integrals: Ba, $\gamma_{6s6s}=\gamma_{6p6p}=\gamma_{6s6p}=4.68$ eV, $\gamma_{5d5d}=5.19$ eV, $\gamma_{5d6s}=\gamma_{5d6p}=3.79$ eV; B, $\gamma=8.68$ eV; O, $\gamma=13.00$ eV. Resonance integrals: Ba, $\beta_{6s}=\beta_{6p}=-2.66$ eV, $\beta_{5d}=-12.50$ eV; B, $\beta=-17.00$ eV; O, $\beta=-34.20$ eV.
[19] R. Pariser, J. Chem. Phys. **24**, 250 (1956).
[20] B. J. Orr and J. Ward, Mol. Phys. **20**, 513 (1971).
[21] S. J. Lalama and A. F. Garito, Phys. Rev. A **20**, 1179 (1979).
[22] R. Frohlich, Z. Kristallogr. **168**, 109 (1984).
[23] R. W. Munn, Mol. Phys. **89**, 555 (1996).
[24] D. A. Kleinman, Phys. Rev. **126**, 1977 (1952).
[25] R. W. Boyd and J. E. Sipe, in *Nonlinear Optics and Optical Physics*, edited by I.-C. Khoo, J. F. Lam, and F. Simoni (World Scientific, Singapore, 1994), p. 104.
[26] D. N. Nikogosyan, Appl. Phys. A: Solids Surf. **52**, 359 (1991).
[27] C. Chen, B. Wu, A. Jiang, and G. You, Sci. Sin. Ser. B **7**, 579 (1984).
[28] Y. Wu, T. Sasaki, S. Nakai, A. Yokotani, H. Tang, and C. Chen, Appl. Phys. Lett. **62**, 2614 (1993).
[29] Y. Mori, I. Kurda, S. Nakajima, T. Sasaki, and S. Nakai, Appl. Phys. Lett. **67**, 1818 (1995).